(V_P) and shear (V_S) wave velocities of MgO along several isotherms (Fig. 3) show that temperature effects decrease with pressure and the velocities of MgO remain comparable to the seismic velocities (*6*) in the upper half of the LM and are slightly larger in the lower half; however, the density of MgO is less than the bulk density of the LM. In the LM, the properties of MgO will be modified by the presence of iron. The wave velocities of magnesiowüstite should be lower than the seismic velocities of the LM, whereas their densities should be comparable (*22–24*).

The seismic parameter, $v = (\partial \ln V_S / \partial \ln V_P)_P$, is a measure of the relative lateral (isobaric) variations in V_S and V_P. Seismic tomography indicates that v increases from ~1.7 from the top of the LM to a value exceeding 3 to the bottom (*24*). To understand whether such lateral heterogeneity can be of thermal origin requires a precise knowledge of v for the component minerals at relevant conditions. High-T experiments at ambient pressures have yielded smaller values for v (<1.5) (*5*). Our calculated T dependence of the velocities constrains v in MgO to vary from ~1.4 at the top to ~1.9 at the bottom of the LM. Earlier PIB calculations estimated v ~ 2.5 at the bottom of the LM (*25*). Our results suggest that unless v is considerably larger in magnesiowüstite or silicate perovskite, the large lateral heterogeneity cannot be attributed to T effects alone if the mantle behaves as a elastic medium during the passage of seismic waves. However, the large seismic value of v may be associated with anelastic effects that affect V_S more strongly than V_P at the low frequencies of seismic waves and high T's (*26*).

References and Notes

1. R. M. Wentzcovitch, J. L. Martins, G. D. Price, *Phys. Rev. Lett.* **70**, 3947 (1993); B. B. Karki *et al.*, *Am. Mineral.* **82**, 635 (1997).
2. G. Fiquet *et al.*, *Phys. Earth Planet. Inter.* **105**, 21 (1998); S. Saxena *et al.*, *Am. Mineral.* **84**, 226 (1999); J. D. Bass, in *Mineral Physics and Crystallography: A Handbook of Physical Constants*, T. Ahrens, Ed. (American Geophysical Union, Washington, DC, 1995), pp. 45–63; O. L. Anderson and G. D. Isaak, in *Mineral Physics and Crystallography: A Handbook of Physical Constants*, T. Ahrens, Ed. (American Geophysical Union, Washington, DC, 1995), pp. 64–97; C. S. Zha *et al.*, *Earth Planet. Sci. Lett.* **159**, 25 (1998).
3. S. V. Sinogeikin and J. D. Bass, *Phys. Rev. B* **59**, 14141 (1999).
4. G. Chen, R. C. Liebermann, D. J. Weidner, *Science* **280**, 1913 (1998).
5. D. G. Isaak, O. L. Anderson, T. Goto, *Phys. Chem. Mineral.* **16**, 704 (1989).
6. A. M. Dziewonski and D. L. Anderson, *Phys. Earth Planet. Inter.* **25**, 297 (1981).
7. E. Matzel, M. K. Sen, S. P. Grand, *Geophys. Res. Lett.* **23**, 2417 (1996); E. J. Garnero and T. Lay, *J. Geophys. Res.* **102**, 8121 (1997); T. Lay, Q. Williams, E. J. Garnero, *Nature* **392**, 461 (1998).
8. S. Karato, *Earth Planets Space* **50**, 1019 (1998); *Pure Appl. Geophys.* **151**, 565 (1998).
9. S. Baroni, P. Giannozzi, A. Testa, *Phys. Rev. Lett.* **58**, 1861 (1987); P. Giannozzi *et al.*, *Phys. Rev. B* **43**, 7231 (1991).
10. Calculations were carried out with the local density approximation (parameterization of J. P. Perdew and A. Zunger [*Phys. Rev. B* **23**, 5048 (1981)]]. Pseudopotentials were generated by the methods of U. von Barth and R. Car (unpublished data) for Mg and N. Troullier and J. L. Martins [*Phys. Rev. B* **43**, 1993 (1991)] for O. The plane wave cutoff was 90 rydbergs, and the Brillouin zone sampling included six special k points for equilibrium and up to 16 points for the strained lattices. Phonon dispersions were determined by diagonalization of the dynamical matrix obtained from linear electron-density response (*9*).
11. A. E. Ringwood, *Composition and Petrology of the Earth's Mantle* (McGraw-Hill, New York, 1975).
12. B. B. Karki *et al.*, *Am. Mineral.* **82**, 51 (1997).
13. The calculated frequencies of Γ_{TO}, Γ_{LO}, X_{TA}, X_{LA}, X_{TO}, X_{LO}, L_{TA}, and L_{TO} phonons are 414, 710, 289, 433, 464, 555, 287, and 371 cm^{-1}, respectively, in agreement with the neutron scattering data of 408, 718, 299, 422, 443, 554, 288, and 369 cm^{-1} at ambient conditions [M. J. L. Sangster *et al.*, *J. Phys. C* **3**, 1026 (1970)]. The equation of state parameters obtained from a fit of free energies to a fourth-order finite strain equation at ambient conditions are volume V_0 = 18.81 Å^3, isothermal bulk modules K_{T0} = 159 GPa, and its pressure derivatives K_{T0}' = 4.30 and K_{T0}'' = −0.030 GPa^{-1}. They agree with the experimental values of V_0 = 18.69 Å^3, K_{T0} = 160 ± 2 GPa, and K_{T0}' = 4.15 determined under hydrostatic conditions (*27*). Our results at 1100 K, V_0 = 19.44 Å^3, K_{T0} = 136 GPa, and K_{T0}' = 4.48 (K_{T0}'' = −0.039 GPa^{-1}), are similar to the experimental values of V_0 = 19.31 Å^3, K_{T0} = 135 ± 3 GPa, and K_{T0}' = 4.2 (*27*). The calculated room temperature density varies from 5.45 to 5.65 g cm^{-3} at 169 to 196 GPa, compared with the shock-wave data of 5.50 to 5.70 g cm^{-3} (*16*).
14. Y. S. Touloukian, R. K. Kirdby, R. E. Taylor, T. Y. R. Lee, *Thermophysical Properties of Matter*, vol. 13 (IFI/Plenum, New York, 1977).
15. The mode Grüneisen parameters, defined as $\gamma_i = -d\ln\omega_i / d\ln V$, where ω_i is frequency, are nearly constant at small volumes and increase rapidly at large volumes. The rapid increase in α at low P's and high T's is related to the rapid increase in γ_i's at large equilibrium volumes.
16. T. S. Duffy and T. Ahrens, *Geophys. Res. Lett.* **20**, 1103 (1993).
17. We determined $c_s = (c_{11} - c_{12})/2$ and c_{44} for which isothermal and adiabatic values are identical by calculating free energies for strained (tetragonal and trigonal) configurations and relating them with the free energy expansion in terms of strains. The isothermal (K_T) and adiabatic (K_S) bulk moduli were determined from the equation of state parameters. Adiabatic (isothermal) c_{11} and c_{12} were then derived from c_s and K_S (K_T).
18. H. A. Spetzler, *J. Geophys. Res.* **75**, 2073 (1970).
19. D. G. Isaak, R. E. Cohen, M. E. Mehl, *J. Geophys. Res.* **95**, 7055 (1990).
20. T. S. Duffy, R. J. Hemley, H. K. Mao, *Phys. Rev. Lett.* **74**, 1371 (1995).
21. For instance, single-crystal polarization anisotropy in shear wave velocity at D″ pressures is ~55% for MgO (*12*), compared with the anisotropy of ~13, 7, 18, and 16% for $MgSiO_3$ perovskite, $CaSiO_3$ perovskite, SiO_2, and CaO, respectively [B. B. Karki and L. Stixrude, *J. Geophys. Res.* **104**, 13025 (1999)].
22. T. S. Duffy and D. L. Anderson, *J. Geophys. Res.* **94**, 1895 (1989).
23. R. Jeanloz and A. B. Thompson, *Rev. Geophys.* **21**, 51 (1983).
24. A. M. Dziewonski and J. H. Woodhouse, *Science* **236**, 37 (1987); S. P. Grand, *J. Geophys. Res.* **99**, 11591 (1994).
25. D. G. Isaak, O. L. Anderson, R. E. Cohen, *Geophys. Res. Lett.* **19**, 741 (1992).
26. S. I. Karato, *Geophys. Res. Lett.* **20**, 1623 (1993).
27. Y. Fei, *Am. Mineral.* **84**, 272 (1999).

28. Supported by NSF grant EAR-9628042 and INFM of Italy. Computing facilities are provided by the Minnesota Supercomputing Institute. We thank S. Karato for useful discussions.

23 July 1999; accepted 20 October 1999

Core Rotational Dynamics and Geological Events

Marianne Greff-Lefftz[1] and Hilaire Legros[2]

A study of Earth's fluid core oscillations induced by lunar-solar tidal forces, together with tidal secular deceleration of Earth's axial rotation, shows that the rotational eigenfrequency of the fluid core and some solar tidal waves were in resonance around 3.0 × 10^9, 1.8 × 10^9, and 3 × 10^8 years ago. The associated viscomagnetic frictional power at the core boundaries may be converted into heat and would destabilize the D″ thermal layer, leading to the generation of deep-mantle plumes, and would also increase the temperature at the fluid core boundaries, perturbing the core dynamo process. Such phenomena could account for large-scale episodes of continental crust formation, the generation of flood basalts, and abrupt changes in geomagnetic reversal frequency.

The precession and nutations of Earth, as well as the secular variation of the length of day, are caused by lunar-solar gravitational torque (*1, 2*). In addition to this spatial motion, there is a tidally induced flow in the fluid core ($\vec{\omega}^c$) (*3*) [which can be observed with the use of superconducting gravimeters and very long baseline interferometry data] and a differential rotation of the inner core with respect to the mantle ($\vec{\omega}^s$) (*4, 5*). These flows may resonate in the vicinity of the nearly diurnal period (*6, 7*), and their amplitudes depend on some geodynamical parameters such as the core flattening, the geodetic constant, and the tidal elastic Love numbers. Here, we calculate the epochs of resonance in the past as a function of Earth's rotation rate, and we investigate the associated dissipative power at the core-mantle boundary (CMB) and at the inner core boundary (ICB).

We use the classical Liouville equations (which describe the conservation of the angular momenta) in a form given by (*5*). This

[1]Department of Geomagnetism and Paleomagnetism, Institut de Physique du Globe de Paris, 4 place Jussieu, 75252 Paris 05, France. [2]Ecole et Observatoire des Sciences de la Terre, 5 rue R. Descartes, 67084 Strasbourg, France.

system includes four rotational eigenmodes: the Chandler wobble (motion of $\vec{\omega}$, Earth's rotation vector, with respect to the figure axis of the mantle, with a period of about 435 days), the inner-core wobble (motion of $\vec{\omega} + \vec{\omega}^s$ with respect to the figure axis of the inner core, with a period of about 2300 days), the free core nutation (FCN), and the free inner core nutation (FICN). The two nutations are nearly diurnal and are denoted λ_{FCN} and λ_{FICN}, respectively. Using complex notation, the equatorial frictional torque acting on the mantle ($\vec{\Gamma}^m$) and on the inner core ($\vec{\Gamma}^s$) can be written as

$$\Gamma_1^m + i\Gamma_2^m = (K_m + iK'_m)A^c\Omega\omega^c$$

$$\Gamma_1^s + i\Gamma_2^s = (K_s + iK'_s)A^s\Omega(\omega^c - \omega^s) \quad (1)$$

where $K_m + iK'_m$ and $K_s + iK'_s$ are frictional constants, depending on the core viscosity and on the conductivity of the inner core, the fluid outer core, and the lower mantle; A^c and A^s are the mean moments of inertia of the fluid outer core and the inner core, respectively; Ω is the sidereal rotation; $\omega^c = \omega_1^c + i\omega_2^c$; $\omega^s = \omega_1^s + i\omega_2^s$; and λ_a is the nearly diurnal frequency of the tesseral degree-two tidal potential (*8*). Because $K_c = K_m + (A^s/A)K_s$ (where A is the mean moment of inertia of Earth), the solutions of the system for the equatorial components of the core's rotation vector are, to first order,

$$R_{CMB}^2 = \frac{b^2}{\Omega^2}[(\omega_1^c)^2 + (\omega_2^c)^2]$$

$$= \frac{x_c^c}{(\lambda_a - \lambda_{FCN})^2 + [(A/A^m)K_c\Omega]^2}$$

$$R_{ICB}^2 = \frac{c^2}{\Omega^2}[(\omega_1^c - \omega_1^s)^2 + (\omega_2^c - \omega_2^s)^2]$$

$$= \frac{x_c^s}{(\lambda_a - \lambda_{FCN})^2 + [(A/A^m)K_c\Omega]^2} + \frac{x_s^s}{(\lambda_a - \lambda_{FICN})^2 + (K_s\Omega)^2} \quad (2)$$

where x_c^c, x_c^s, and x_s^s are tidal coefficients, b and c are the outer core and inner core radii, and A^m is the mean moment of inertia of the mantle. The power extracted from the rotational kinetic energy of Earth is dissipated by resistivity in the magnetic diffusion layers and by viscosity in the Ekman layer at the CMB and the ICB (*9*):

$$P_{CMB} = -\vec{\Gamma}^m \cdot \vec{\omega}^c = -A^c\Omega K_m[(\omega_1^c)^2 + (\omega_2^c)^2]$$

$$P_{ICB} = -\vec{\Gamma}^s \cdot (\vec{\omega}^c - \vec{\omega}^s) = -A^s\Omega K_s[(\omega_1^c - \omega_1^s)^2 + (\omega_2^c - \omega_2^s)^2] \quad (3)$$

The equatorial rotations ω^c and ω^s are in resonance when the frequency of the excitation is equal to the eigenfrequency of the system, as for any externally forced harmonic oscillator (Eq. 2). Here, the frequency of the excitation source (tidal potential) is nearly diurnal and is thus close to the FCN. Because of the secular deceleration of Earth's rotation, the temporal evolution of the flattening of the core, and the inner core's growth, the FCN period varies slowly with time. Consequently, there are times in the past when $\lambda_a = \lambda_{FCN}$, meaning that a resonance between λ_a and λ_{FCN} had occurred; sometimes the amplitude of the differential rotation of the core with respect to the mantle may have been large, depending on the frictional constants (*7, 10*).

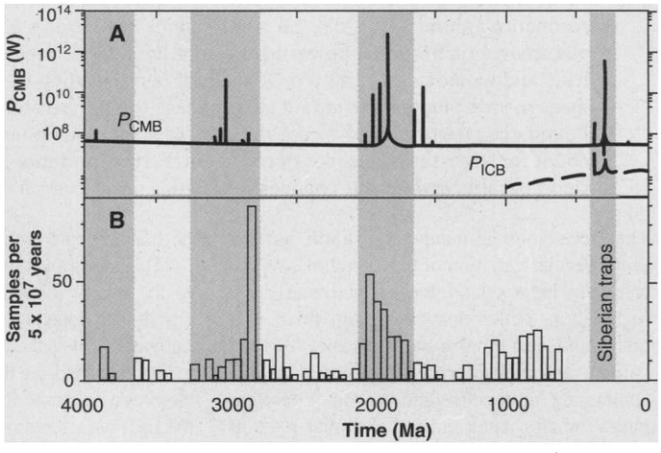

Fig. 1. (**A**) Temporal evolution of the viscomagnetic dissipative power at the CMB (P_{CMB}, solid line) and at the ICB (P_{ICB}, dashed line) induced by the nearly diurnal lunar-solar tidal potential. The uncertainties on the resonance dates increase in the geological past. The secular trend corresponds essentially to the viscomagnetic dissipative power induced by the lunar-solar precession ($\lambda_a = -\Omega$), which varies with time because of the secular deceleration of Earth's axial rotation. Note that the energy associated with a resonance (about 5×10^{25} J) is larger than the energy accumulated by the precession during 4 Ga (about 4×10^{24} J for our conductivity model). (**B**) Frequency distribution of U-Pb zircon dates from Precambrian igneous rocks [from three geographic areas of figure 10 of (*17*)]. All dates correspond to igneous crystallization, and the occurrence frequency may be interpreted as the rate of worldwide crustal production.

To compute these resonance times, we need a model for the tidal secular deceleration of Earth and for the growth of the inner core. The secular deceleration of Earth's axial rotation and the evolution of the distance between the moon and Earth result from the braking torque due to lunar tidal forces acting on Earth (*11*). Following earlier studies on the temporal evolution of the Earth-moon system (*12*), we used a linear model of Earth's axial rotation between 4 Ga and the present, with average deceleration rates of about -3.90×10^{-22} rad/s^2 from 4 Ga to 500 Ma and -5.98×10^{-22} rad/s^2 from 500 Ma to the present (where 1 Ga = 10^9 years ago and 1 Ma = 10^6 years ago). The deceleration rate depends on the friction at the bottom of the oceans related to the paleogeographical time modifications. Consequently, we assume uncertainties at the level of 5% on these average deceleration rates.

The FCN depends on the hydrostatic flattening of the core and on the geodetic constant, both of which vary as the square of the sidereal rotation. The contribution of the nonhydrostatic flattening of the core (due to the mantle density heterogeneity varying on convection time scales) is assumed to be ±5% with respect to the hydrostatic flattening. The period of the FCN is not perturbed by the presence of the solid inner core (less than 1 day in the sidereal period because $A^s/A \ll 1$) (*5*), and consequently the resonance dates are not sensitive to models of inner core growth (*13*). This is not the case for the amplitude of the inner core oscillation or for the dissipative power at the ICB. Here, we use a model constructed by (*13*) for the growth of the inner core since 1 Ga. We have also taken into account the secular variations of the lunar-solar tidal forces (*14*).

With these constraints, we calculated time intervals (lasting 200 million or 300 million years) of resonances induced by tidal waves in the past. We computed the amplitude of the oscillation of the fluid outer core with respect to the mantle and that of the inner core with respect to the fluid outer core from Eq. 2. The viscomagnetic dissipative power P_{CMB} and P_{ICB} (in watts), for a frictional constant K_c of 1.5×10^{-7} [that is, for a lower mantle conductivity of about 10 $(\text{ohm}\cdot\text{m})^{-1}$ within a 2000-km-thick layer and an Ekman number of about 10^{-15} within the fluid outer core (*15*)], shows four times of resonance (shaded area in Fig. 1A) around 3.8 Ga, 3.0 Ga, 1.8 Ga, and 300 Ma. For each group, the maximum amplification of the dissipative power is associated with a solar tidal wave such as $\lambda_a = -[\Omega + (k\Omega_o/366.25)]$, where Ω_o is the present sidereal rotation and k takes values of 1 to 4, respectively, for the annual, semiannual, 1/3-annual, and 1/4-annual, waves related to the elliptical motion of Earth with respect to the sun.

From Eq. 2, both core motion and the dissipative power at the CMB are inversely proportional to K_c at the time of resonance. For $K_c = 1.5 \times 10^{-7}$, there is a resonance amplification factor of about 10^4 with respect to the present value of the dissipative power: P_{CMB} may reach a few terawatts at the time of resonance; that is, it may have the same order of magnitude as the estimates for the present heat flux from the core to the mantle, which ranges from 10^{12} W to 9×10^{12} W (*2*). By time integration of the dissipative power, we compute the energy associated with a resonance event to be about 5×10^{25} J.

During times of resonance, the frictional power may be converted into heat (by ohmic heating and viscous friction) and destabilize the D″ thermal layer, leading to the generation of deep-mantle plumes. With a lag time between the time of resonance and the surface observations (*16*), these plumes may be responsible for continental flood basalt volcanism (such as the Siberian traps at 250 Ma) and may play a role in the formation of the continental crust in the Archaean or Proterozoic. The two major resonances between 4 Ga and 500 Ma occurred around 3 ± 0.2 Ga and 1.8 ± 0.2 Ga, for the 1/3-annual and semi-annual tidal waves (shaded area in Fig. 1). These dates correspond to peaks in worldwide crustal production (Fig. 1B) (*17, 18*); thus, it seems possible to correlate the Precambrian resonance times with major crust-forming episodes. The temperature near the ICB would increase during resonance periods. This effect could stop inner core growth (which may be responsible for the present dynamo processes) and lead to a new momentum equilibrium for the geodynamo. The temperature increase at the ICB may also enhance thermal convection within the fluid core, perturbing the fluid equilibrium.

One consequence of the core's dynamic seen at Earth's surface would be a change in the geomagnetic field, possibly changing the magnetic field reversal frequency. Consequently, we try to compare the times of major resonances with the geomagnetic field reversal frequency (*19*). Since 500 Ma, one correlation appears: The resonance of the annual solar tidal wave occurred at the end of the Kiamen Reverse Superchron (270 Ma) and may have restarted the reversal process. Simultaneously, this resonance destabilizes the D″ region, and 20 million years later, plumes arrived at Earth's surface from D″, producing widespread volcanism (Siberian traps) and mass extinction (Permo-Triassic limit).

References and Notes

1. P. Melchior, *Physique et Dynamique Planétaires, Géodynamique* (Vander, Brussels, 1973), vol. 4.
2. F. D. Stacey, *Physics of the Earth* (Brookfield, Brisbane, Australia, ed. 3, 1992).
3. H. Poincare, *Bull. Astron.* **27**, 321 (1910).
4. P. M. Mathews, B. A. Buffet, T. A. Herring, I. I. Shapiro, *J. Geophys. Res.* **96**, 8219 (1991).
5. V. Dehant, J. Hinderer, H. Legros, M. Lefftz, *Phys. Earth Planet. Inter.* **76**, 259 (1993).
6. A. Toomre, *Geophys. J. R. Astron. Soc.* **38**, 335 (1974).
7. J. Hinderer and H. Legros, in *Structure and Dynamics of Earth's Deep Interior,* D. E. Smylie and R. Hide, Eds. (AGU Geophys. Monogr. 46, 1988), pp. 79–82.
8. F. Roosbeek, *Geophys. J. Int.* **126**, 197 (1996).
9. D. E. Loper, *Phys. Earth Planet. Inter.* **11**, 43 (1975).
10. G. Williams, *Earth Planet. Sci. Lett.* **128**, 155 (1994).
11. K. Lambeck, *The Earth's Variable Rotation* (Cambridge Univ. Press, Cambridge, 1980).
12. M. N. Ross and G. Schubert, *J. Geophys. Res.* **94**, 9533 (1989).
13. S. Labrosse, J. P. Poirier, J. L. Le Mouel, *Phys. Earth Planet. Inter.* **99**, 1 (1997).
14. To compute the tidal potential in the past, we have taken into account the temporal evolution of the lunar-solar frequency (using the Kepler law and the Lagrange equations) and of the amplitude of the lunar potential (which varies as $1/d^3$, where d is the Earth-moon distance). An estimation of the temporal evolution of the removal of the moon is obtained from the conservation of the angular momentum of the Earth-moon system restricted to the axial rotation of Earth and to the orbital revolution of the moon.
15. J. P. Poirier, *Geophys. J. Int.* **92**, 99 (1988).
16. The change in the behavior of the dynamo precedes the surface events by a lag time equal to the sum of the length of time it takes the plume to erupt from the D″ layer after the resonance (that is, the characteristic time of the D″ layer responses to a thermal signal from the core) plus the length of time it takes the plume to rise to the surface.
17. K. C. Condie, *Palaeogeogr. Palaeoclimatol. Palaeoecol.* **75**, 57 (1989).
18. S. R. Taylor and S. M. McLennan, *The Continental Crust: Its Composition and Evolution* (Blackwell, Oxford, 1985).
19. J. G. Ogg, *Global Earth Physics, A Handbook of Physical Constants* (AGU Reference Shelf 1, T. J. Ahrens, Ed., 1995), pp. 240–265.

20. We thank S. Gilder for discussions and remarks on the original manuscript.

3 August 1999; accepted 20 October 1999

Eight Centuries of North Atlantic Ocean Atmosphere Variability

David E. Black,[1]* Larry C. Peterson,[1] Jonathan T. Overpeck,[2]† Alexey Kaplan,[3] Michael N. Evans,[3] Michaele Kashgarian[4]

Climate in the tropical North Atlantic is controlled largely by variations in the strength of the trade winds, the position of the Intertropical Convergence Zone, and sea surface temperatures. A high-resolution study of Caribbean sediments provides a subdecadally resolved record of tropical upwelling and trade wind variability spanning the past 825 years. These results confirm the importance of a decadal (12- to 13-year) mode of Atlantic variability believed to be driven by coupled tropical ocean-atmosphere dynamics. Although a well-defined interdecadal mode of variability does not appear to be characteristic of the tropical Atlantic, there is evidence that century-scale variability is substantial. The tropical Atlantic may also have been involved in a major shift in Northern Hemisphere climate variability that took place about 700 years ago.

Although short-term variability in Atlantic climate is thought to be relatively well understood (*1*), both the patterns and the mechanisms of variability on decadal to century scales are as yet poorly known. In the southern Caribbean, the anoxic Cariaco Basin is well positioned to provide century- to millennium-length histories of trade wind–induced coastal upwelling (Fig. 1) as well as surface ocean changes that result from variations in the large-scale circulation of the Atlantic (*2–4*). Varved high-deposition-rate sediments [up to >100 cm per thousand years (ky)] and an abundance of microfossils result in one of the few marine records capable of preserving evidence of interannual- to century-scale climate variability in the tropical Atlantic. Between January and March, when the Intertropical Convergence Zone (ITCZ) moves close to the equator, strong easterly trade winds along the coast of Venezuela create intense Ekman upwelling and peak primary productivity over the Cariaco Basin and the continental margin (*3*, *5*). Beginning in June or July, as the ITCZ moves north to a position near the Venezuelan coast, the trade winds diminish, and upwelling over the basin weakens. Studies of Cariaco Basin microplankton have shown that local populations dominated

[1]Rosenstiel School of Marine and Atmospheric Science, University of Miami, Miami, FL 33149, USA. [2]National Oceanic and Atmospheric Administration Paleoclimatology Program and the Institute for Arctic and Alpine Research, University of Colorado, Boulder, CO 80309, USA. [3]Lamont-Doherty Earth Observatory, Columbia University, Palisades, NY 10964, USA. [4]Center for Accelerator Mass Spectrometry, Lawrence Livermore National Laboratory, Livermore, CA 94551, USA.

*Present address: Department of Geological Sciences, University of South Carolina, Columbia, SC 29208, USA.

†Present address: Institute for the Study of Planet Earth, Department of Geosciences, University of Arizona, Tucson, AZ 85721, USA.